Supplemental Materials

Supplemental Table 1. Probesets increased in m19z and m1928z vs m19-musBBz CAR T cells.

Supplemental Table 2. Probesets increased in m19-musBBz vs m19z and m1928z CAR T cells.

Supplemental Table 3. Probesets differentially expressed in m19z vs m19-musBBz CAR T cells.

Supplemental Table 4. Probesets differentially expressed in m1928z vs m19-musBBz CAR T cells.

Supplemental Methods

Gene Expression

Microarray. For m19z, m1928z and m19-musBBz comparison, three million CAR T cells were incubated with 3×10^5 3T3-mCD19 cells overnight. The next day live CAR T cells were sorted into Trizol (Thermo Fisher Scientific, Waltham, MA). RNA was isolated according to manufacturer's instructions and run on a MOE 430A 2.0 array Mouse Genechip (Affymetrix, Santa Clara, CA) at the Genomics Core Facility. Gene expression analyses and graphic representations were performed with the Partek Genomics Suite Software. RMA normalization was performed and values generated for each probeset for all samples. Differentially expressed genes were detected by ANOVA and probesets of statistical significance were defined by a-fold change > 2 and a FDR ≤ 0.05.

RNA-SEQ. For m19z, m1928z and m19-humBBz comparison, three million CAR T cells were incubated with 1×10^6 3T3-mCD19 cells for 48 hr. Live CD4+ CAR T cells were sorted into Trizol. RNA was isolated according to manufacturer's instructions and evaluated for quality. The Genomic Core performed mRNA enrichment and cDNA library preparation using the Illumina Tru-seq stranded mRNA sample prep kit. Final RNA-seq libraries were reviewed for size and quality on the Agilent TapeStation, followed by quantitative PCR-based quantitation with the Kapa Library Quantification Kit. The libraries sequenced on two NextSeq high-output 2x75 paired-end sequencing runs in order to generate approximately 40 million pairs of reads per sample. Sequence reads were aligned to the human reference genome in a splice-aware fashion using Tophat2 (1), allowing for accurate alignments of sequences across introns. Aligned reads were quantitated at the gene level using HTseq (2). Normalization, expression modeling, and difference testing were performed using DESeq (3). Quality control measures included custom scripts and RSeqC (4) to examine read count metrics, alignment fraction, chromosomal

alignment counts, expression distribution measures, and principle components analysis and hierarchical clustering.

Differentially expressed genes were detected by ANOVA and probesets of statistical significance were defined by a-fold change > 4 and a FDR ≤ 0.01. Gene set enrichment analysis was performed (on the gene expression values) to analyze the enrichment of the gene sets using GSEA software (http://www.broadinstitute.org/gsea/index.jsp). C5 collection version v6.0 from the Molecular Signature Database (MSigDB v6.0 C5), which contains the expert-curated gene ontology (GO) gene sets, were used in the analysis. We used vertebrate homology resource (http://www.informatics.jax.org/homology.shtml) to convert between homologues human and mouse genes. For all comparisons, data was collapsed to gene symbols. 1000 permutations based on gene sets were performed. Gene sets were ranked according to false discovery rate (FDR) q-value. At the default FDR q-value cut-off within GSEA of 0.25, we identified 3 gene sets that are upregulated in m19z and 68 gene sets upregulated in m1928z.

Microarray and RNA-SEQ data have been submitted to GEO (Gene Expression Omnibus) with the accession number GSE112567.

CD33-targeted CARs

Anti-CD33 antibodies were developed at the Vanderbilt Antibody and Protein Resource using standard methods (5). Briefly, after completing a series of immunizations splenocytes of immunized mice were isolated and fused to a non-Ig secreting myeloma cell line and grown in a semi-solid plate. Antibody-secreting clusters were identified in semi-solid plates and selected for clonal expansion in 96 well plates.

During expansion supernatant was collected and assayed for CD33 binding by ELISA as well as flow cytometry. Based on this screening hybridomas were selected for expansion and isolation of RNA, which was used to amplify IgH and IgL rearrangements. Based on the IgH and IgL rearrangements scFv were designed and cloned into the NcoI/NotI sites of our human CD19-targeted CAR in the SFG retroviral cassette. This allowed replacement of the anti-human CD19 scFv with anti-human CD33 scFv. These constructs were then used to produce gammaretroviral supernatant as described in Methods.

In vivo NALM6 animal model of CD19-targeted CAR T cells

The NALM6 leukemia mouse model has been described (6). Briefly, NALM6-GL cells were i.v. injected to NSG mice at $5x10^5$ dose. Four days later, mice were treated with $3x10^5$-$1x10^6$ human CD19 targeted CAR T cells. Human CD19 targeted CAR T cells with excess TRAF2 were made by CAR and mouse TRAF2 co-transduction or transduction with a bicistronic construct combining CAR and human TRAF2. Blood samples were collected weekly for flow cytometry. Leukemia burden was evaluated weekly using bioluminescence imaging on an IVIS system. Survival was monitored. Mice were sacrificed when they develop signs of progressive leukemia.

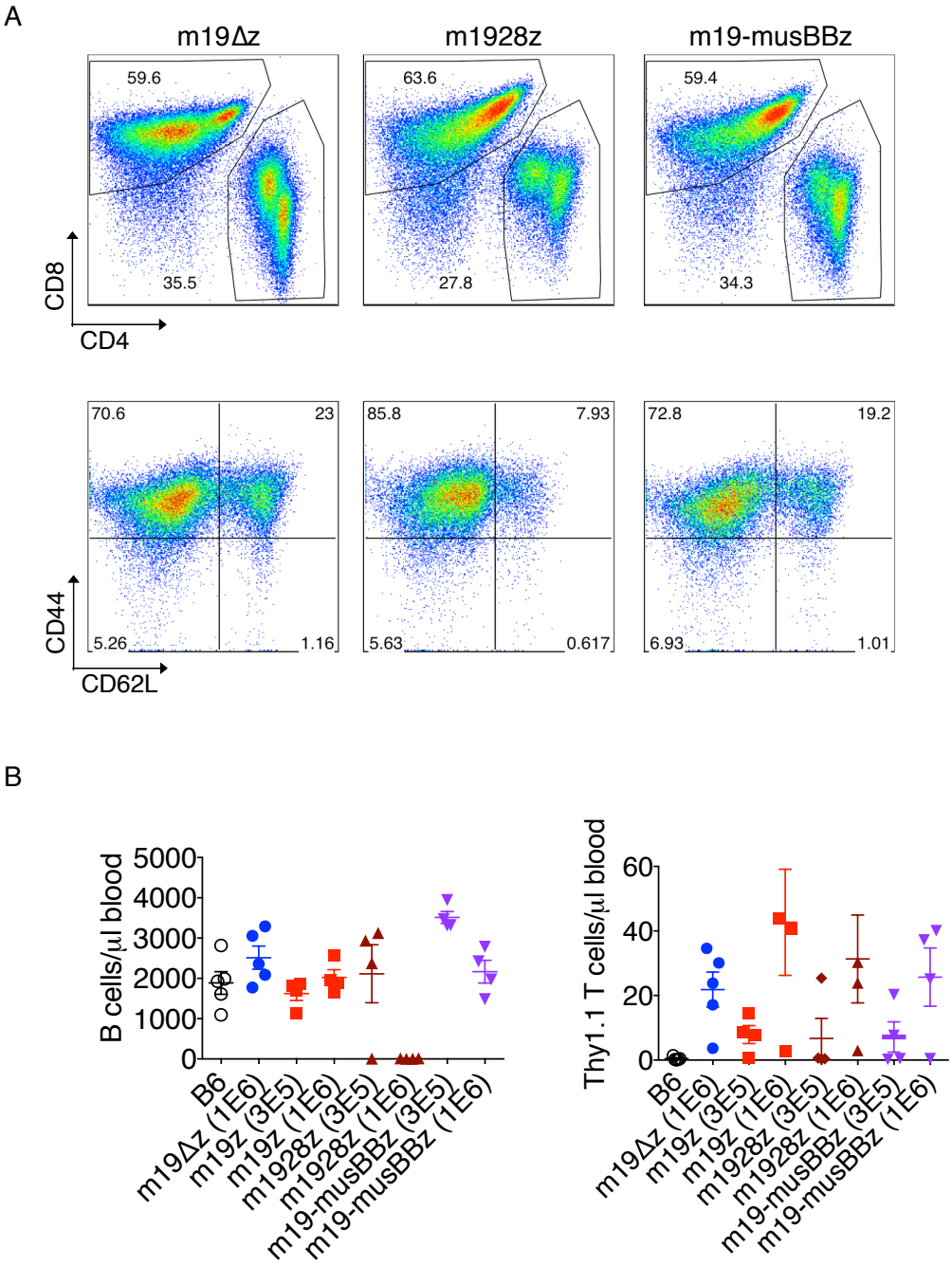

Supplemental Figure 1. Immune phenotype of mCD19 targeted CAR T and dose titration of in vivo efficacy. (A) Immune phenotype of transduced T cells used in $5x10^6$ dose in vivo study (Figure 1C&D). Cells were pre-gated on single live cells. **(B)** In vivo B cell killing and T cell persistence with T cell dose titration. After Eμ-ALL injection, different doses of T cells were given to 300 mg/kg CTX pre-conditioned mice. B (B220+CD19+) and T (CD3+Thy1.1+) cells in peripheral blood were quantitated 3 weeks after CAR T injection. Each dot indicates one mouse. Data are from one single experiment (n=34 total).

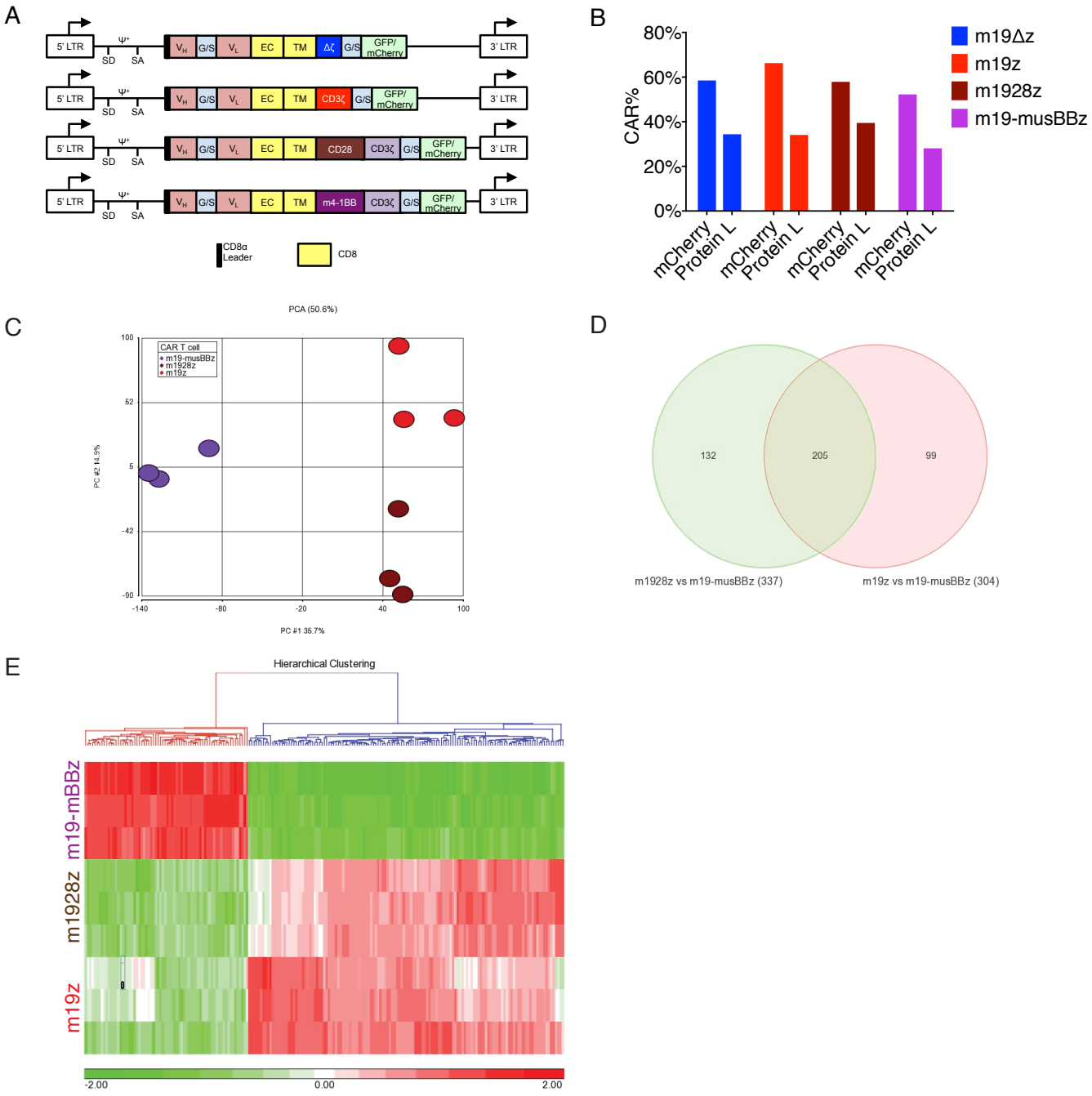

Supplemental Figure 2. Gene expression of fluorescent-protein tagged CAR T cells. (A) Schematic of genetic constructs for mCD19 targeted CARs. Shown are the long terminal repeats (LTR), packaging signal Ψ, splice donor (SD), splice acceptor (SA), V_H and V_L regions of the scFv (single-chain variable fragment), the extracellular hinge (EC), transmembrane (TM), and intracellular regions of the retroviral construct. G/S, (Gly4Ser1)3 linker sequence. **(B)** Comparison of fluorescence protein and Protein L as a method to evaluate CAR expression. One million T cells transduced with mCherry-tagged CARs were incubated with 1 µg Biotin-Protein L and then fluochrome-conjugated streptavidin. Cells were subjected to flow cytometry. Data are representative of 4 independent experiments. **(C)** Principal component

analysis (PCA) of mCD19-targeted CAR T cells stimulated with antigen. **(D)** Venn Diagram demonstrating the number of genes differentially expressed (n=205) in m19-musBBz CAR T cells compared to both m19z and m1928z CAR T cells. **(E)** A heatmap of the 205 differentially expressed genes. The list of 205 genes is included in Supplemental Tables 1-4. For (C)-(E), CAR T cells with the m19z, m1928z, or m19-musBBz CAR tagged to the fluorescent protein GFP were incubated with 3T3-mCD19 AAPC at 10:1 E:T ratio overnight, FACS-sorted, and lysed to isolate RNA. Each group of CAR T cells was transduced, stimulated, and sorted independently in triplicates.

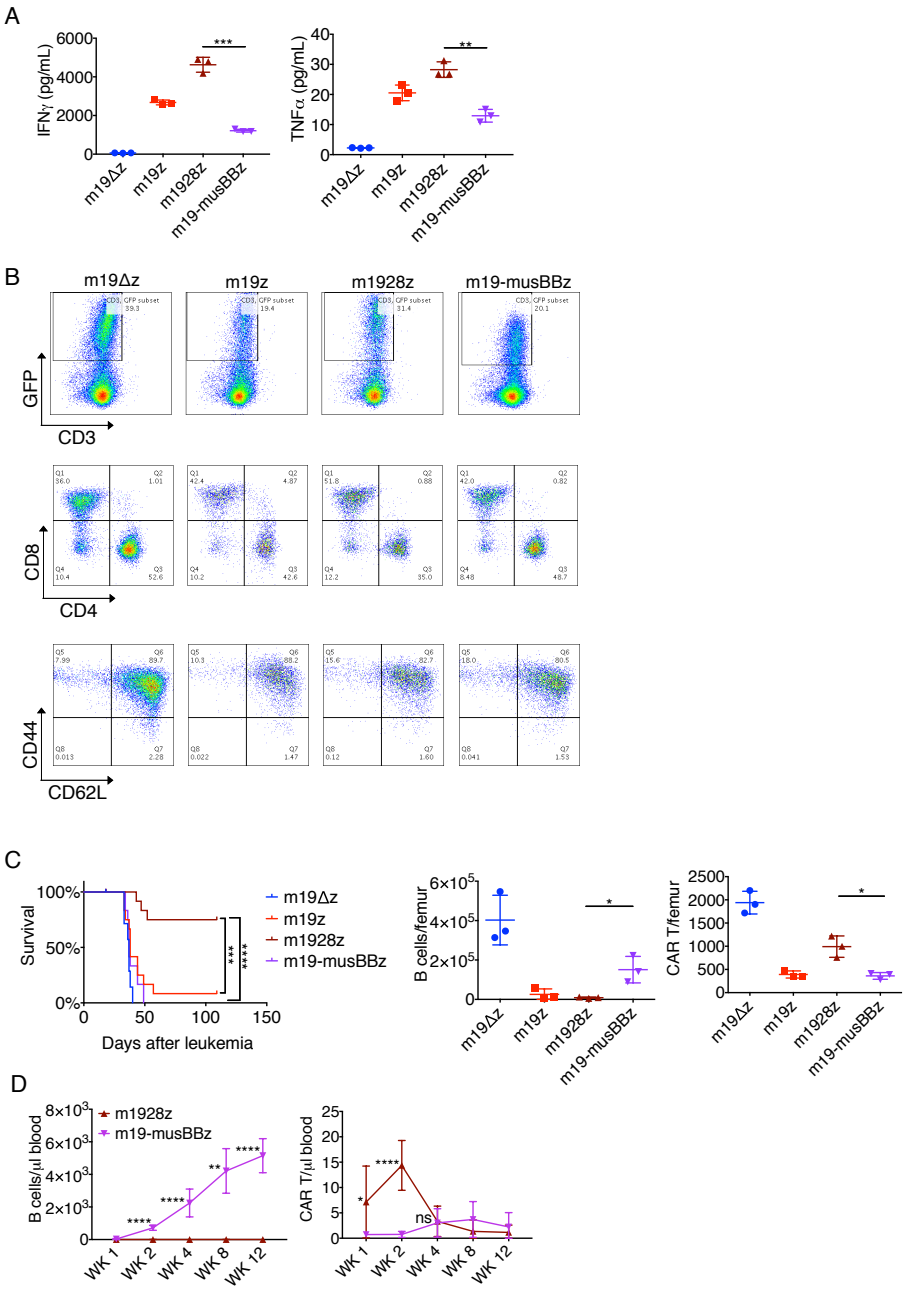

Supplemental Figure 3. Fluorescent protein tagged CAR T cells function similarly to non-tagged counterparts. (A) Cytokines released by fluorescent protein tagged CAR T cells upon antigen stimulation. Day 4 CAR T cells were co-cultured with 3T3-mCD19 at 10:1 ratio for 24 hr. Supernatant was subjected to luminex assay for IFNγ and TNFα. **(B)** Immune phenotype of CAR T cells with a fluorescent protein tag. Day 4 CAR T cells were harvested, beads removed and subjected to flow cytometry. Cells were pre-gated on single live cells (top) or CD3+CAR+ cells (middle & bottom). **(C)** Survival (n=50), in vivo B cell killing and CAR T persistence in mice treated by CAR T cells with a fluorescent protein tag. Seven days after i.v. injection with $1X10^6$ Eμ-ALL cells, mice were i.p. injected with CTX at 250 mg/kg and then one day later i.v. injected with $1X10^6$ CAR T cells. Survival was monitored. BM was isolated 11 days after CAR T injection and subjected to flow cytometry. B (B220+CD19+) and CAR T (CD3+- CAR+) cells were counted using CountBright beads. Each dot indicates one mouse (n=3 per group). Data are from one single experiment. **(D)** B and CAR T cell counts over time in the blood after CAR T treatment. B6 mice were injected with CTX (250 mg/kg) and CAR T cells ($3X10^5$). Blood samples were collected over time and B and CAR T cell numbers were measured by flow cytometry (n=10 per group). Survival curve, logrank test; all other data, unpaired t test. *p<0.05; **p<0.01; ***p<0.001; ****p<0.0001; ns, not significant.

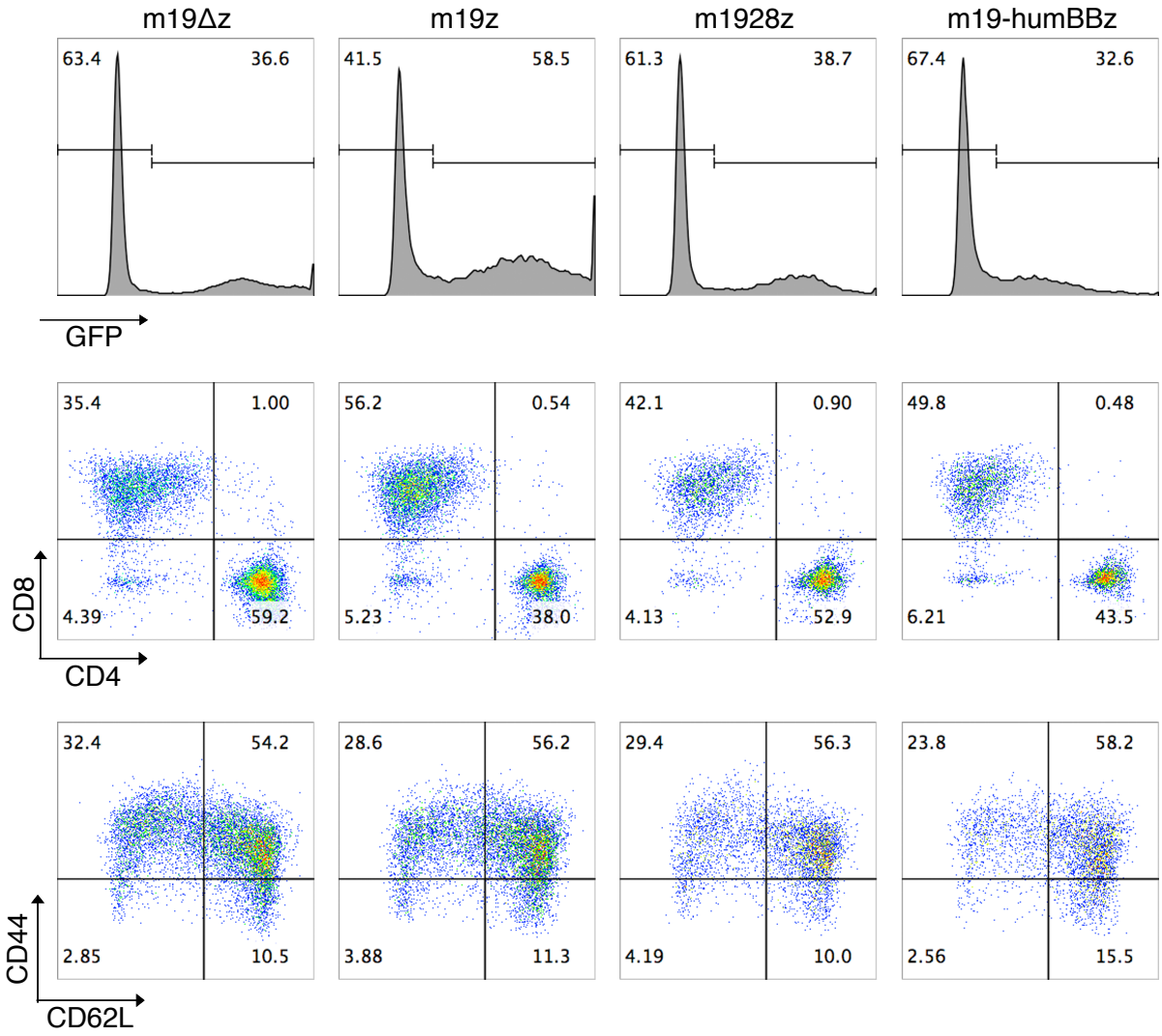

Supplemental Figure 4. Transduction efficiency and immune phenotype of mCD19 targeted CAR T cells for survival study (Figure 2D). Data are representative of four independent productions used to generate CAR T cells for the survival experiments of Figure 2D. For transduction efficiency (top panel), cells were pre-gated on single live cells. For immune phenotype (middle and bottom panels), cells were pre-gated on single live CAR T (CD3+CAR+) cells.

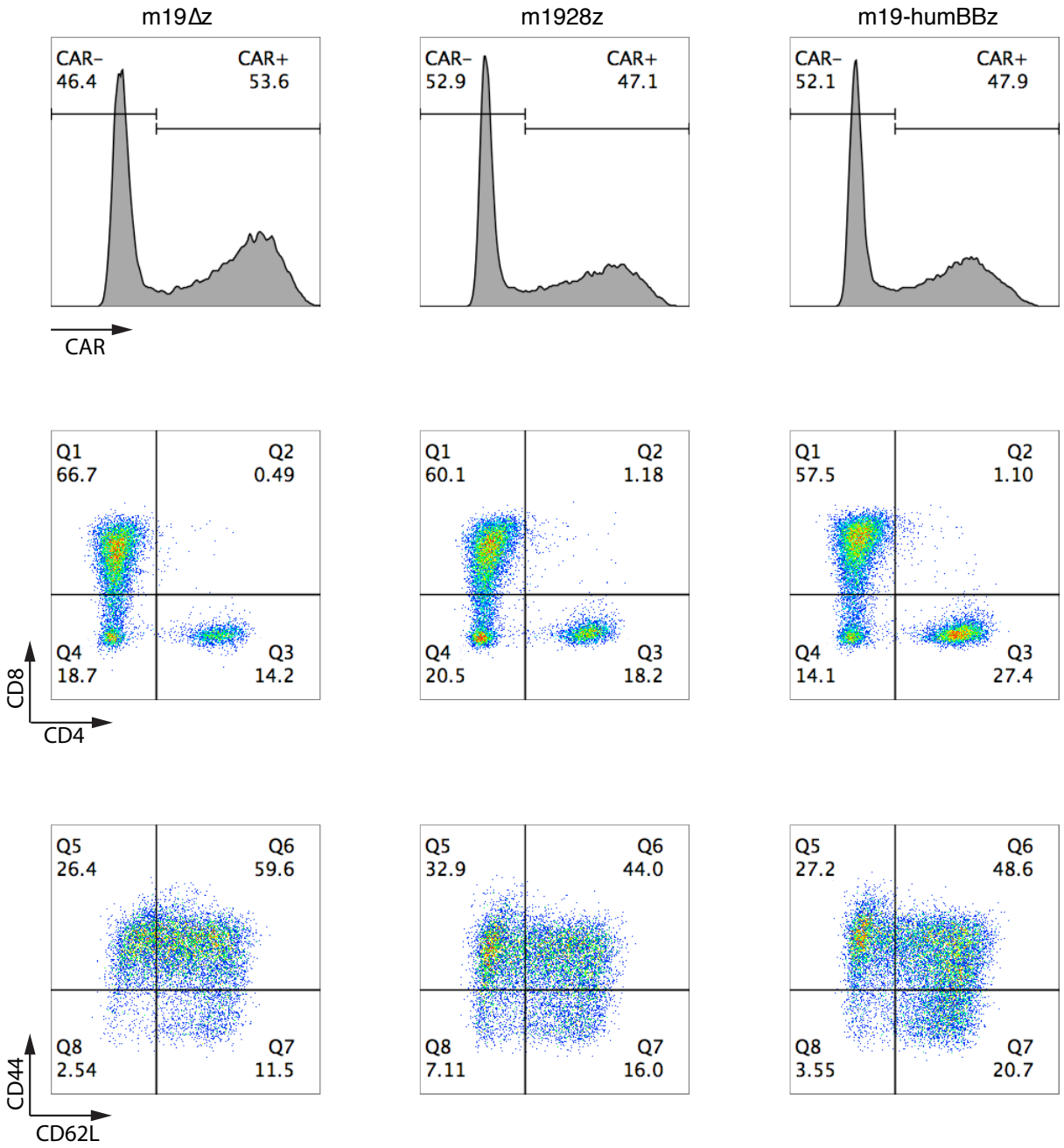

Supplemental Figure 5. Transduction efficiency and immune phenotype of CAR T cells used in irradiated CAR T study (Figure 3B-3C). Day 4 transduced cells were harvested, beads removed, stained with antibodies and subjected to flow cytometry. For transduction efficiency (Top panels), cells were pre-gated on single live cells. For immune phenotype (middle and bottom panels), cells were pre-gated on CD3+CAR+ cells.

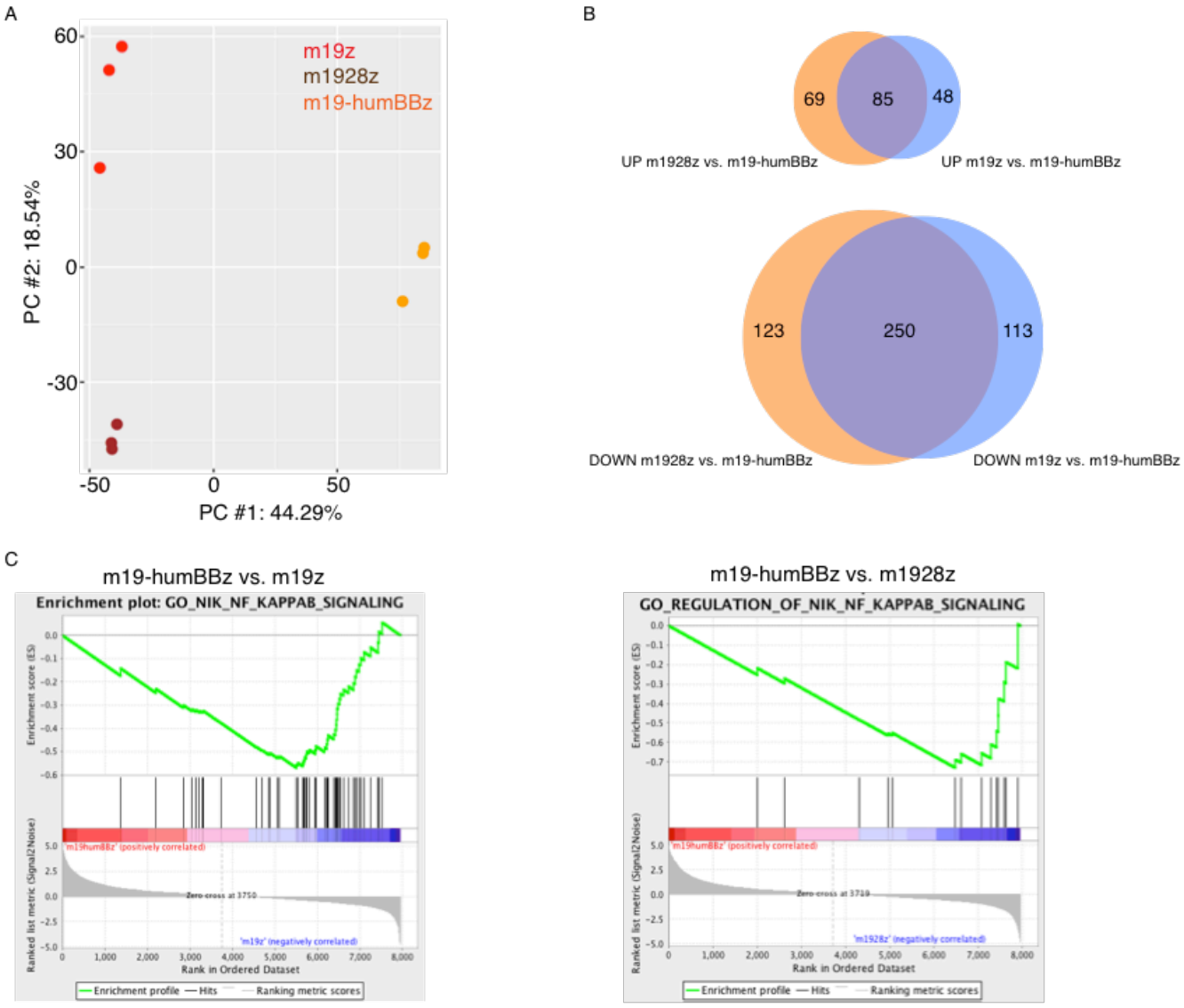

Supplemental Figure 6. Differential gene expression of CD4+ m19-humBBz CAR T cells. T cells with the m19z, m1928z, or m19-humBBz CAR were incubated with 3T3-mCD19 AAPC at 10:1 E:T ratio, FACS-sorted, and lysed to isolate RNA. Each group of CAR T cells was transduced, stimulated, and sorted independently in biologic triplicates. **(A)** PCA of mouse CD19-targeted CAR T cells stimulated with antigen. **(B)** Venn Diagram demonstrating the number of genes differentially expressed in m19-humBBz CAR T cells compared to m19z and m1928z CAR T cells. **(C)** GSEA demonstrates gene sets correlating to NF-κ B regulatory pathways are differentially expressed in m19-humBBz CAR T cells versus m19z or m1928z CAR T cells.

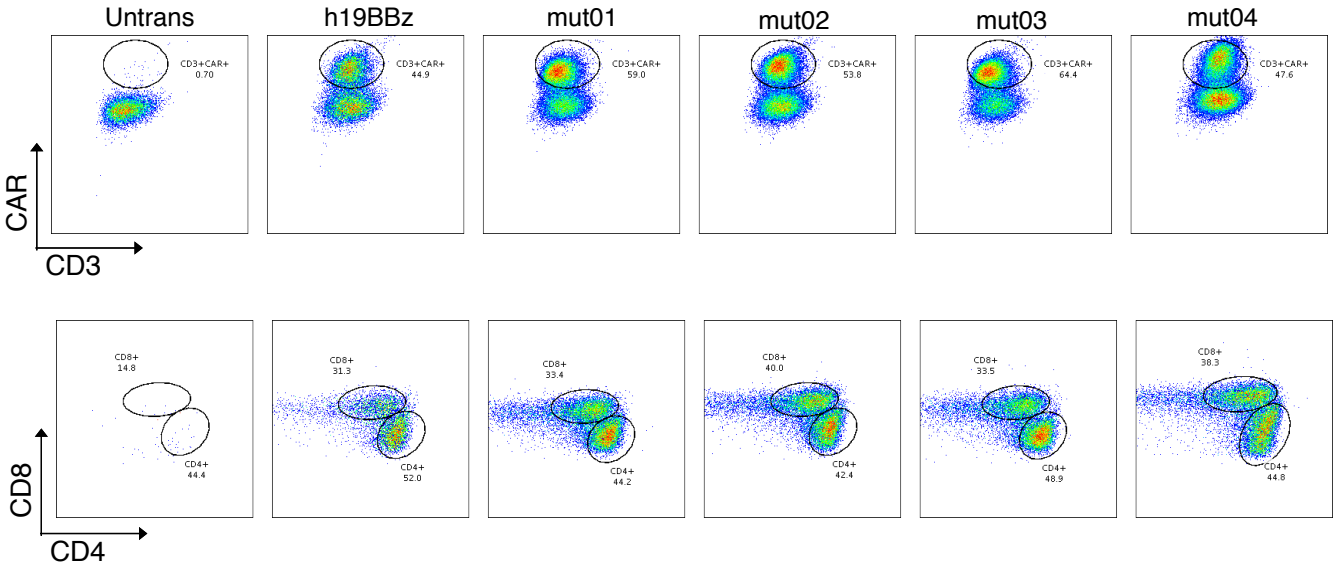

Supplemental Figure 7. CAR expression and CD4/CD8 subsets of human CD19 targeted CAR T cells for Figure 5E-G. For CAR expression (top), cells were pre-gated on single live cells. For immune phenotype (bottom), cells were pre-gated on CD3+CAR+ cells.

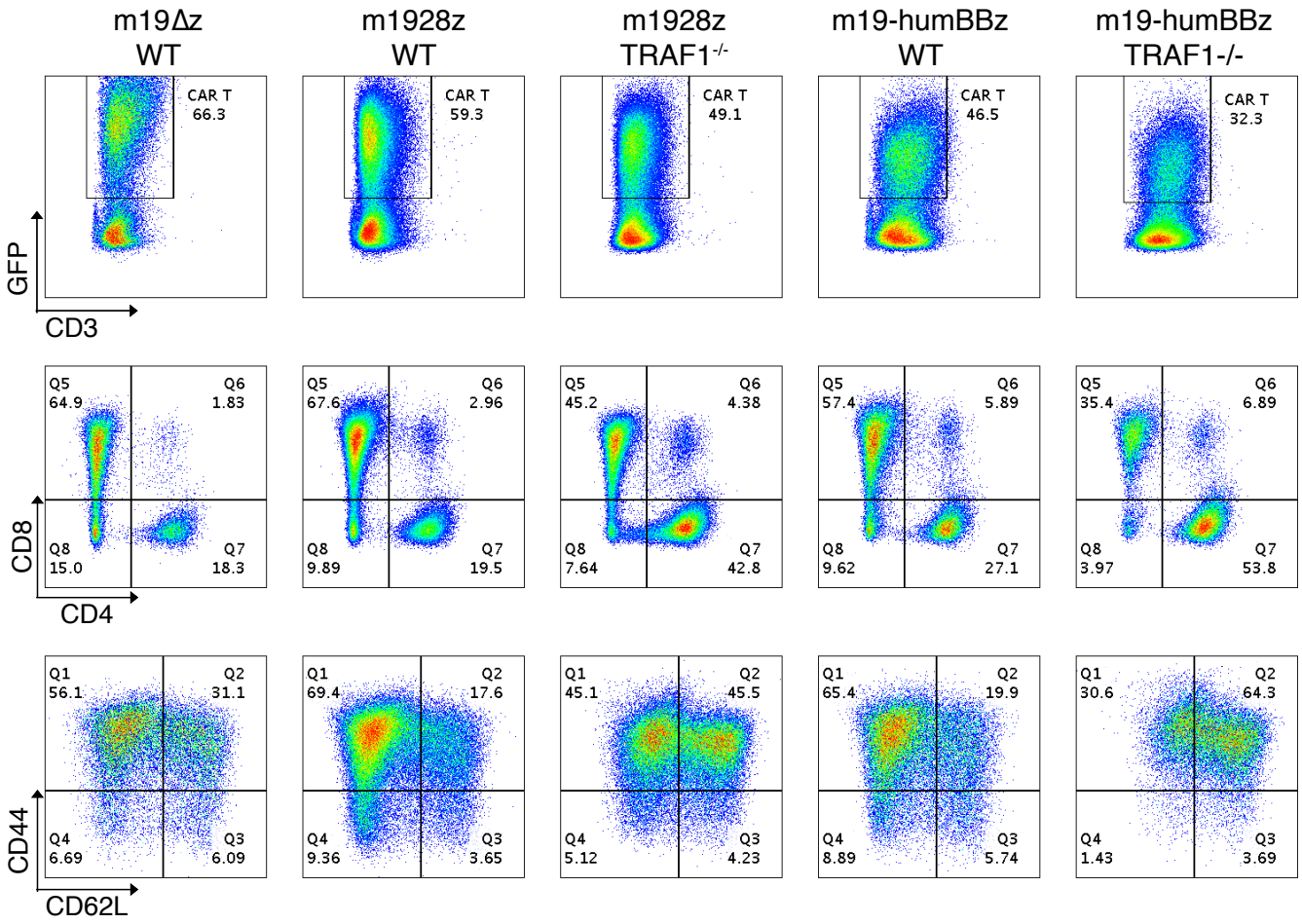

Supplemental Figure 8. Transduction efficiency and immune phenotype of mCD19 targeted wild type (WT) and *Traf1*$^{-/-}$ CAR T cells used for in vivo study (Figure 6D). Day 4 transduced cells were harvested, beads removed, stained with antibodies and subjected to flow cytometry. For transduction efficiency (top panel), cells were pre-gated on single live cells. For CD4/CD8 subsets (middle panel) and memory subsets (bottom panel) cells were pre-gated on single live CAR T (CD3+CAR+) cells.

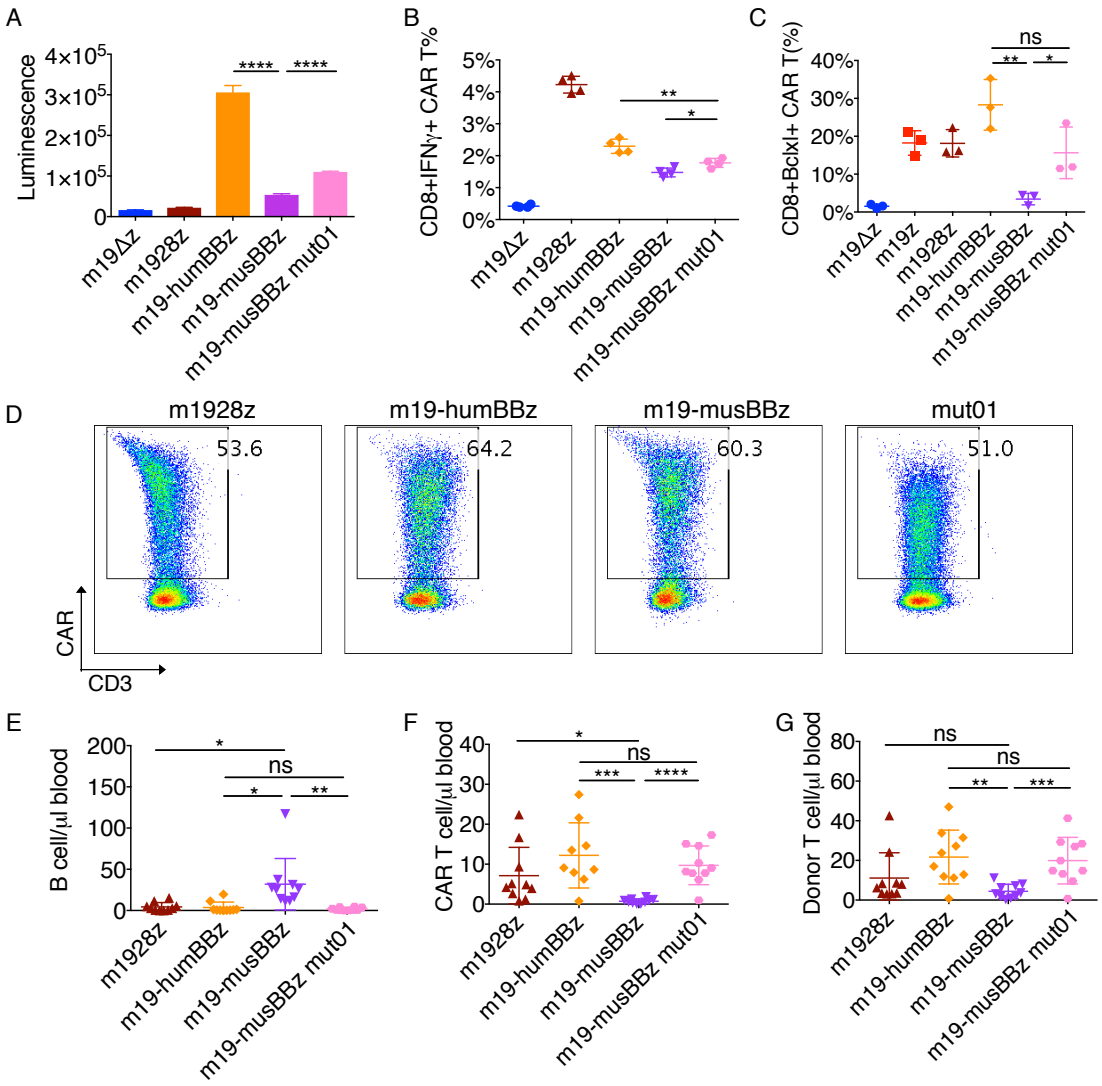

Supplemental Figure 9. Mutated m19-musBBz CAR T cells have increased NF-κ B signaling, improved cytokine production, anti-apoptosis, and in vivo function. (A) NF-κ B signaling in mCD19 targeted CAR T cells. CAR T cells derived from NF-κ B-RE-luc transgenic mice were co-cultured with 3T3-mCD19 for 4 hr. Cell lysates were prepared and subjected to a luciferase assay. Bioluminescence was measured and correlates to NF-κ B signaling. Data are representative of three independent experiments. **(B)** Intracellular IFNγ and **(C)** BCL-XL expression in CD8+ CAR T cells stimulated with 3T3-mCD19. Data are representative of two independent experiments done in triplicate. **(D)** CAR expression in T cells used for in vivo study below. Cells were pre-gated on single live cells. **(E)** B cells (CD19+B220+) in the blood 1 week after CAR T cells injection. **(F)** CAR T cells (CD3+GFP+) in the blood 1 week after CAR T cells injection. **(G)** Donor T cells (CD3+Thy1.1+) in the blood 1 week after CAR T cells injection. (E-G) Each dot indicates one mouse (n=10 per group). Bar graph shown as mean ± SD. All data, unpaired t test. *p<0.05; **p<0.01; ***p<0.001; ****p<0.0001; ns, not significant.

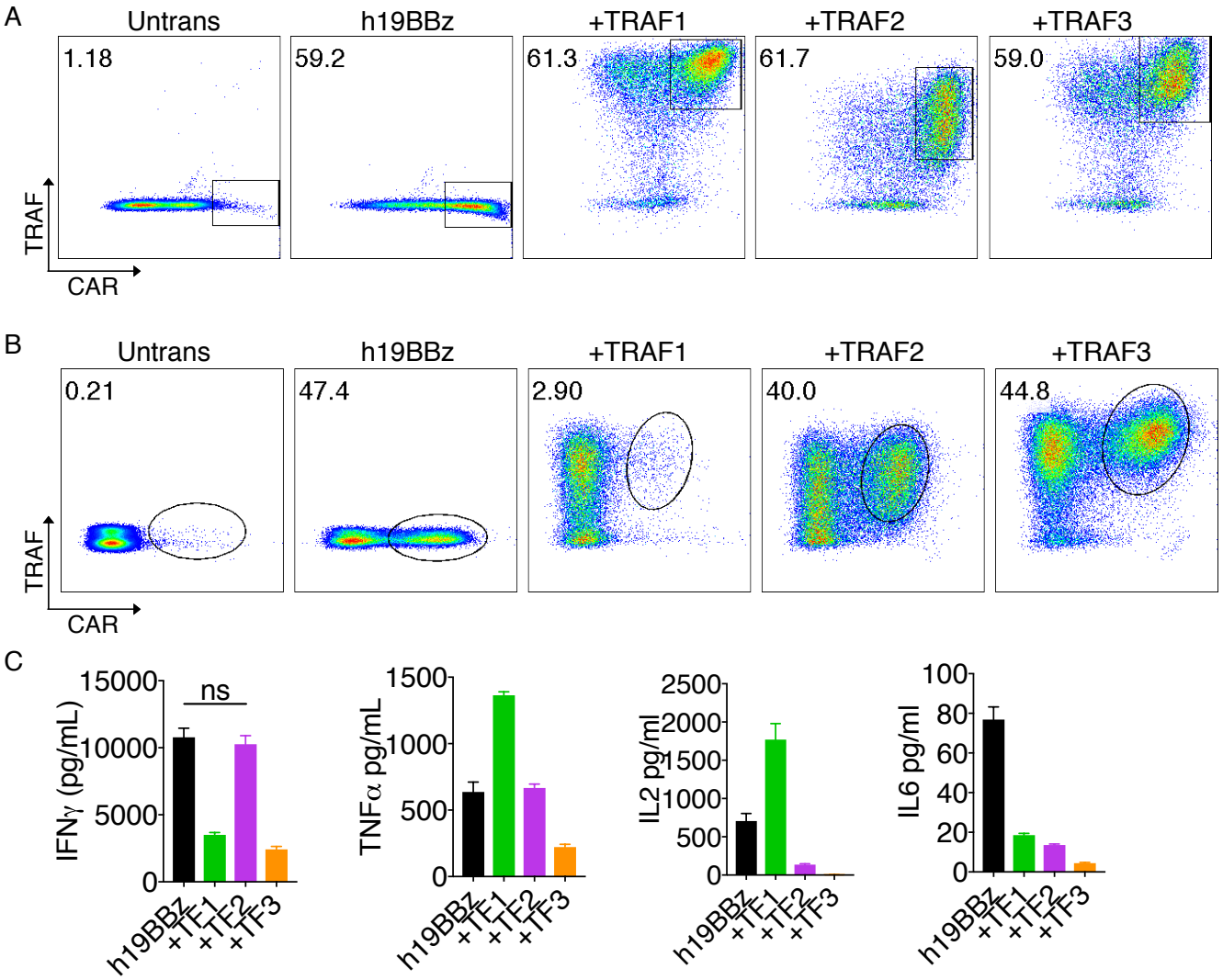

Supplemental Figure 10. TRAF and CAR co-expression in human CD19-targeted CAR T cells. (A) CAR and TRAF expression in hCD19 targeted CAR T cells before antigen stimulation for viability, proliferation, and cytotoxicity assays (Figure 7B-D). Cells were pre-gated on single live cells. Data are one representative of 3 healthy donors. **(B)** CAR and TRAF expression in hCD19 CAR T cells 3 days after stimulation with 3T3-hCD19. Cells were pre-gated on single live cells. Data are from one experiment in triplicate. Numbers indicate percentages of gated cells. **(C)** Cytokine production. CAR T cells were activated on 3T3-hCD19 at 10:1 ratio. After 24 hr supernatant were harvested and cytokines were measured by ELLA. Bar graphs shown as mean ± SD. Data are one representative of 3 different healthy donors in triplicate. All data, unpaired t test. ns, not significant.

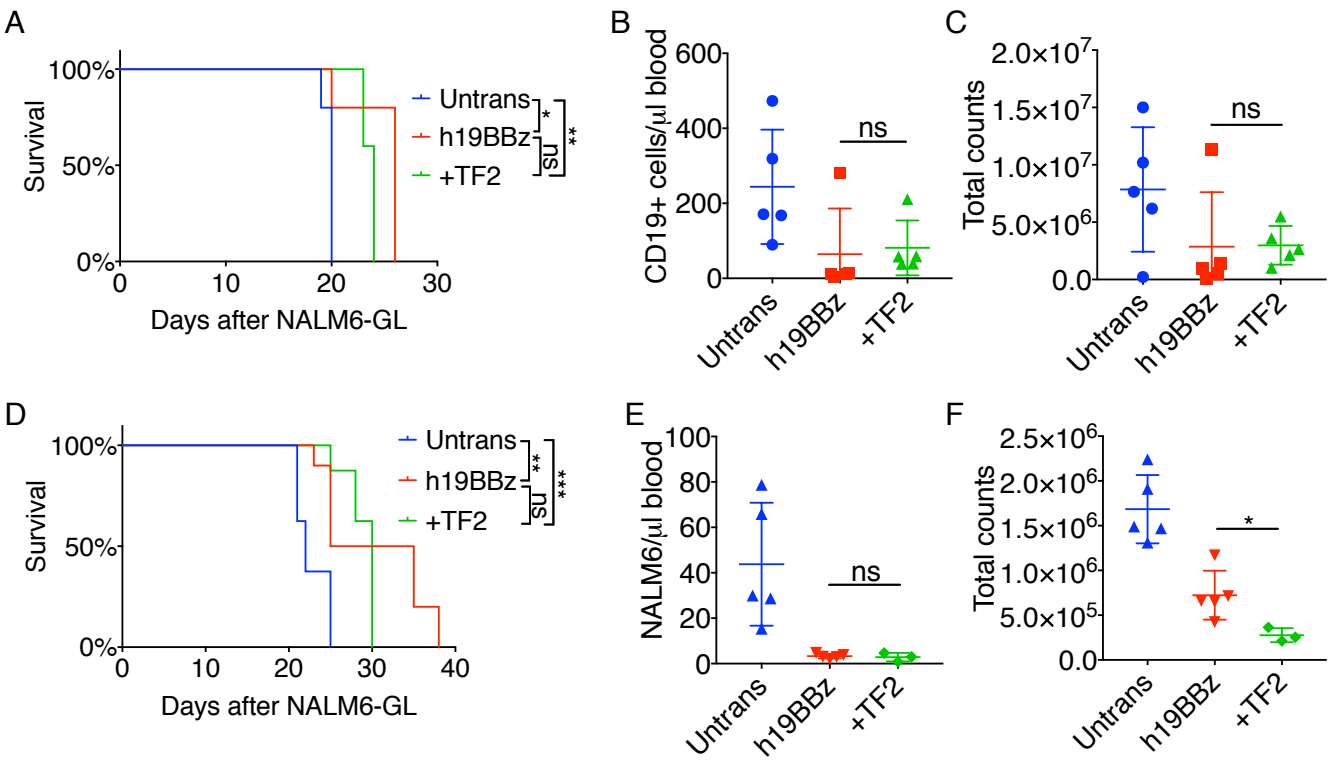

Supplemental Figure 11. TRAF2 over-expressed h19BBz CAR T cells show similar in vivo efficacy to h19BBz CAR T cells in an aggressive leukemia model. NSG mice were implanted with leukemia by i.v. injecting $5x10^5$ NALM6-GL cells. Four days later, mice were i.v. injected with $3x10^5$-$1x10^6$ CAR T cells. Blood samples were collected weekly. Leukemia burden was evaluated weekly using bioluminescence imaging. Survival was monitored. For (A-C), TRAF2 was co-transduced to make CAR T cells, n=15 total, and data are from one experiment. For (D-F), a bicistronic construct expressing CAR and TRAF2 was transduced to make CAR T cells. Survival data are pooled from two independent experiments (n=26), and counts are from one experiment. Each dot indicates a mouse. Survival curve, logrank test; all other data, unpaired t test. *$p<0.05$; **$p<0.01$; ns, not significant.

Supplemental Table 1. Probesets increased in m19z and m1928z vs. m19-musBBz CAR T cells

Probeset ID	Gene Symbol	Fold-Change	Probeset ID	Gene Symbol	Fold-Change
1418679_at	Gzmf	8.0	1422601_at	Serpinb9	2.9
1422668_at	Serpinb9b	7.8	1417523_at	Plek	2.9
1419561_at	Ccl3	6.9	1450495_a_at	Klrk1	2.9
1450297_at	Il6	6.8	1423101_at	Paqr4	2.9
1416842_at	Gstm5	6.5	1431724_a_at	P2ry12	2.9
1420789_at	Klra5	5.1	1422887_a_at	Ctbp2	2.8
1448390_a_at	Dhrs3	4.9	1424356_a_at	Metrnl	2.8
1453060_at	Rgs8	4.9	1417434_at	Gpd2	2.7
1449835_at	Pdcd1	4.8	1421188_at	Ccr2	2.7
1448942_at	Gng11	4.8	1424711_at	Tmem2	2.7
1422867_at	Gzmg	4.8	1420343_at	Gzmd	2.6
1450650_at	Myo10	4.8	1448328_at	Sh3bp2	2.6
1416714_at	Irf8	4.7	1419814_s_at	S100a1	2.6
1416666_at	Serpine2	4.6	1423543_at	Swap70	2.6
1420398_at	Rgs18	4.6	1421186_at	Ccr2	2.6
1448452_at	Irf8	4.5	1450871_a_at	Bcat1	2.6
1423231_at	Nrgn	4.4	1420344_x_at	Gzmd	2.6
1423319_at	Hhex	4.4	1420388_at	Prss12	2.6
1422544_at	Myo10	4.3	1427985_at	Spin4	2.6
1426318_at	Serpinb1b	4.3	1449852_a_at	Ehd4	2.5
1425947_at	Ifng	4.3	1436584_at	Spry2	2.5
1449991_at	Cd244	4.1	1448562_at	Upp1	2.5
1451862_a_at	Prf1	4.1	1428077_at	Tmem163	2.5
1420788_at	Klrg1	4.1	1422880_at	Sypl	2.5
1451584_at	Havcr2	4.1	1449799_s_at	Pkp2	2.5
1424099_at	Gpx8	4.0	1422879_at	Sypl	2.4
1426169_a_at	Lat2	4.0	1450140_a_at	Cdkn2a	2.4
1422804_at	Serpinb6b	4.0	1449164_at	Cd68	2.4
1449570_at	Klrb1c	3.9	1449383_at	Adssl1	2.4
1450750_a_at	Nr4a2	3.9	1417753_at	Pkd2	2.4
1448749_at	Plek	3.8	1420159_at	Myo1e	2.4
1449965_at	Mcpt8	3.8	1422881_s_at	Sypl	2.4
1449254_at	Spp1	3.7	1417588_at	Galnt3	2.4
1426063_a_at	Gem	3.7	1421317_x_at	Myb	2.4
1428034_a_at	Tnfrsf9	3.7	1450646_at	Cyp51	2.3
1422837_at	Scel	3.7	1422734_a_at	Myb	2.3
1417335_at	Sult2b1	3.6	1432459_a_at	Zbtb32	2.3
1450171_x_at	Gzme	3.6	1450194_a_at	Myb	2.3
1418317_at	Lhx2	3.6	1419091_a_at	Anxa2	2.3

1421256_at	Gzmc	3.6	1417178_at	Gipc2	2.3
1451021_a_at	Klf5	3.6	1434705_at	Ctbp2	2.3
1433741_at	Cd38	3.5	1423596_at	Nek6	2.3
1434025_at	---	3.4	1426334_a_at	Bcl2l11	2.3
1428379_at	Slc17a6	3.4	1417400_at	Rai14	2.3
1417749_a_at	Tjp1	3.4	1452011_a_at	Uxs1	2.2
1425470_at	LOC105247125	3.4	1422255_at	Kcna4	2.2
1421688_a_at	Ccl1	3.4	1418026_at	Exo1	2.2
1421227_at	Gzmd	3.3	1424966_at	Tmem40	2.2
1426037_a_at	Rgs16	3.3	1432410_a_at	Bmp7	2.2
1449888_at	Epas1	3.3	1425785_a_at	Txk	2.2
1418610_at	Slc17a6	3.3	1416304_at	Litaf	2.2
1448748_at	Plek	3.2	1416303_at	Litaf	2.2
1418340_at	Fcer1g	3.2	1431422_a_at	Dusp14	2.2
1425125_at	Oit3	3.2	1451122_at	Gm38481	2.2
1460469_at	Tnfrsf9	3.2	1450131_a_at	Bspry	2.2
1424588_at	Srgap3	3.1	1451318_a_at	Lyn	2.1
1417936_at	Ccl9	3.1	1426001_at	Eomes	2.1
1449856_at	Rgs18	3.1	1421048_a_at	Ypel1	2.1
1426120_a_at	Cd244	3.1	1431782_s_at	Ypel1	2.1
1426808_at	Lgals3	3.1	1422477_at	Cables1	2.1
1419647_a_at	Ier3	3.1	1434427_a_at	Rnf157	2.1
1452492_a_at	Slc37a2	3.0	1426171_x_at	Klra7	2.1
1416431_at	Tubb6	3.0	1435086_s_at	Klhdc2	2.1
1419412_at	Xcl1	3.0	1422557_s_at	Mt1	2.1
1418910_at	Bmp7	2.9	1423804_a_at	Gm38481	2.1
1450136_at	Cd38	2.9	1430394_a_at	Abcb9	2.1
1426911_at	Dsc2	2.9	1450290_at	Pdcd1lg2	2.0
1451458_at	Tmem2	2.9			

Supplemental Table 2. Probesets increased in m19-musBBz vs. m19z and m1928z CAR T cells

Probeset ID	Gene Symbol	Fold-Change	Probeset ID	Gene Symbol	Fold-Change
1423100_at	Fos	14.0	1453678_at	Mbd1	2.5
1448830_at	Dusp1	4.6	1449049_at	Tlr1	2.5
1423756_s_at	Igfbp4	4.3	1419695_at	St8sia1	2.4
1459884_at	Cox7c	4.1	1437658_a_at	Snord22	2.4
1433863_at	Btf3	4.0	1419418_a_at	Morc1	2.4
1452519_a_at	Zfp36	4.0	1448656_at	Cacnb3	2.4
1459885_s_at	Cox7c	3.9	1456266_at	Gm5481	2.4
1436882_at	Ubl5	3.7	1436686_at	Zfp706	2.4
1427351_s_at	Ighm	3.6	1456603_at	Fam101b	2.3
1417394_at	Klf4	3.6	1442745_x_at	Gm39971	2.3
1428585_at	Actn1	3.5	1448325_at	Ppp1r15a	2.3
1433471_at	Tcf7	3.4	1425919_at	Ndufa12	2.3
1437405_a_at	Igfbp4	3.4	1442744_at	Gm39971	2.3
1416107_at	Nsg2	3.4	1419694_at	St8sia1	2.3
1420161_at	LOC105245295	3.3	1441023_at	Eif2s2	2.3
1425086_a_at	Slamf6	3.3	1418741_at	Itgb7	2.3
1427329_a_at	Ighm	3.2	1456386_at	Rbm39	2.3
1428283_at	Cyp2s1	3.1	1448327_at	Actn2	2.3
1435290_x_at	H2-Aa	3.1	1420088_at	Nfkbia	2.3
1450461_at	Tcf7	3.1	1451731_at	Abca3	2.3
1422134_at	Fosb	3.0	1421214_at	Cmah	2.3
1448890_at	Klf2	2.9	1449815_a_at	Ssbp2	2.3
1449216_at	Itgae	2.9	1427615_at	Itga4	2.3
1438076_at	Gm5481	2.9	1446147_at	Gm39971	2.2
1417409_at	Jun	2.9	1418128_at	Adcy6	2.2
1442494_at	C79242	2.8	1438211_s_at	Dbp	2.2
1428357_at	Tdrp	2.7	1436871_at	Srsf7	2.2
1423555_a_at	Ifi44	2.6	1437390_x_at	Stx1a	2.2
1426640_s_at	Trib2	2.6	1435316_at	Psma6	2.2
1449731_s_at	Nfkbia	2.6	1438675_at	Sfswap	2.2
1449025_at	Ifit3	2.6	1427335_at	Tmem260	2.2
1421194_at	Itga4	2.6	1446148_x_at	Gm39971	2.2
1448306_at	Nfkbia	2.5	1454703_x_at	Snhg1	2.2
1420659_at	Slamf6	2.5	1449858_at	Cd86	2.2
1438398_at	Rbm39	2.5	1448420_a_at	Fbxl12	2.1

Supplemental Table 3. Probesets differentially expressed in m19z vs. m19-musBBz CAR T cells

Probeset ID	Gene Symbol	Fold-Change	Probeset ID	Gene Symbol	Fold-Change
1437279_x_at	Sdc1	9.1	1449903_at	Crtam	2.3
1426260_a_at	Ugt1a1	5.2	1417300_at	Smpdl3b	2.3
1425471_x_at	LOC105247125	5.0	1452565_x_at	---	2.3
1425538_x_at	Ceacam1	4.8	1426541_a_at	Endod1	2.3
1418547_at	Tfpi2	4.5	1423418_at	Fdps	2.2
1415943_at	Sdc1	4.5	1422748_at	Zeb2	2.2
1427038_at	Penk	4.5	1449184_at	Pglyrp1	2.2
1420421_s_at	Klrb1b	4.2	1452661_at	Tfrc	2.2
1426261_s_at	Ugt1a1	4.1	1424650_at	Pdia5	2.2
1451446_at	Antxr1	3.8	1417162_at	Tmbim1	2.2
1418186_at	Gstt1	3.7	1422123_s_at	Ceacam1	2.2
1448898_at	Ccl9	3.5	1422533_at	Cyp51	2.2
1421578_at	Ccl4	3.4	1460678_at	Klhdc2	2.2
1426182_a_at	Klrc1	3.3	1460682_s_at	Ceacam1	2.2
1425923_at	Mycn	3.3	1459903_at	Sema7a	2.2
1455423_at	Khdc1a	3.3	1452404_at	Phactr2	2.2
1452367_at	Coro2a	3.2	1437330_at	Lrrk1	2.1
1416156_at	Vcl	3.1	1423590_at	Napsa	2.1
1455265_a_at	Rgs16	3.1	1426542_at	Endod1	2.1
1429159_at	Itih5	3.1	1448752_at	Car2	2.1
1428574_a_at	Chn2	3.0	1454904_at	Mtm1	2.1
1451452_a_at	Rgs16	3.0	1418206_at	Sdf2l1	2.1
1425675_s_at	Ceacam1	2.9	1438165_x_at	Vat1	2.1
1418084_at	Nrp1	2.8	1417100_at	Cd320	2.1
1427630_x_at	Ceacam1	2.8	1418401_a_at	Dusp16	2.1
1438312_s_at	Ltbp3	2.8	1427005_at	Plk2	2.1
1425436_x_at	Klra3	2.8	1421933_at	Cbx5	2.1
1429183_at	Pkp2	2.7	1426543_x_at	Endod1	2.1
1425005_at	Klrc1	2.7	1450651_at	Myo10	2.1
1422967_a_at	Tfrc	2.7	1449911_at	Lag3	2.1
1448944_at	Nrp1	2.7	1425469_a_at	LOC105247125	2.1
1418879_at	Fam110c	2.6	1433443_a_at	Hmgcs1	2.0
1430419_at	---	2.6	1428942_at	Mt2	2.0
1424783_a_at	Ugt1a1	2.6	1452539_a_at	Cd247	2.0
1415964_at	Scd1	2.6	1423413_at	Ndrg1	2.0
1450494_x_at	Ceacam1	2.6	1425179_at	Shmt1	2.0
1450790_at	Tg	2.6	1415811_at	Uhrf1	2.0
X00686_5_at	---	2.6	1418350_at	Hbegf	2.0
1425745_a_at	Tacc2	2.6	1449152_at	Cdkn2b	2.0

1428573_at	Chn2	2.6	1460353_at	Ndc1	2.0
1422067_at	Klrb1b	2.5	1449482_at	Hist3h2ba	-2.0
1418449_at	Lad1	2.5	1420404_at	Cd86	-2.0
1426300_at	Alcam	2.5	1423169_at	Taf7	-2.0
1426472_at	Zfp52	2.5	1425518_at	Rapgef4	-2.2
1449481_at	Slc25a13	2.4	1420805_at	Myl10	-2.2
1418049_at	Ltbp3	2.4	1436677_at	1810032O08Rik	-2.3
1448943_at	Nrp1	2.4	1424800_at	Enah	-2.3
X57349_5_at	Tfrc	2.4	1417483_at	Nfkbiz	-2.4
1450296_at	Klrb1a	2.3	1417928_at	Pdlim4	-2.4
1422639_at	Calcb	2.3			

Supplemental Table 4. Probesets differentially expressed in m1928z vs. m19-musBBz CAR T cells

Probeset ID	Gene Symbol	Fold-Change	Probeset ID	Gene Symbol	Fold-Change
1449280_at	Esm1	5.2	1423851_a_at	Shisa2	2.1
1422824_s_at	Eps8	3.8	1456098_a_at	Elmo2	2.1
1439036_a_at	Atp1b1	3.6	1420407_at	Ltb4r1	2.1
1419594_at	Ctsg	3.6	1451944_a_at	Tnfsf11	2.1
1422823_at	Eps8	3.3	1452478_at	Alpk2	2.1
1426680_at	Sepn1	3.1	1416846_a_at	Pdzrn3	2.1
1421654_a_at	Lmna	3.0	1418685_at	Tirap	2.1
1420463_at	Clnk	2.9	1421642_a_at	Cysltr2	2.1
1422280_at	Gzmk	2.9	1421525_a_at	Naip5	2.1
1428572_at	Basp1	2.8	1422041_at	Pilrb1	2.0
1425503_at	Gcnt2	2.8	1425733_a_at	Eps8	2.0
1434868_at	4933431E20Ri	2.7	1418057_at	Tiam1	2.0
1423530_at	Stk32c	2.7	1460192_at	Osbpl1a	2.0
1450989_at	Tdgf1	2.7	1453915_a_at	Slc37a3	2.0
1427918_a_at	Rhoq	2.7	1418943_at	Zak	2.0
1424089_a_at	Tcf4	2.7	1455570_x_at	Cnn3	-2.0
1434148_at	Tcf4	2.6	1450484_a_at	Cmpk2	-2.0
1428197_at	Tspan9	2.6	1420089_at	Nfkbia	-2.0
1450792_at	Tyrobp	2.6	1436836_x_at	Cnn3	-2.0
1448590_at	Col6a1	2.6	1424378_at	Ldlrap1	-2.0
1451867_x_at	Arhgap6	2.5	1426043_a_at	Capn3	-2.0
1431226_a_at	Fndc4	2.5	1425065_at	Oas2	-2.0
1419184_a_at	Fhl2	2.5	1438397_a_at	Rbm39	-2.0
1423852_at	Shisa2	2.4	1421922_at	Sh3bp5	-2.1
1415973_at	Marcks	2.4	1419135_at	Ltb	-2.1
1430826_s_at	Gcnt2	2.4	1438215_at	Srsf3	-2.1
1449170_at	Piwil2	2.4	1455220_at	Frat2	-2.1
1456700_x_at	Marcks	2.4	1436994_a_at	Hist1h1c	-2.1
1416318_at	Serpinb1a	2.4	1426997_at	Thra	-2.1
1449456_a_at	Cma1	2.4	1431388_at	Mphosph10	-2.1
1451733_at	Gcnt2	2.4	1450783_at	Ifit1	-2.1
1419083_at	Tnfsf11	2.3	1417395_at	Klf4	-2.1
1455901_at	Chpt1	2.3	1452844_at	Pou6f1	-2.1
1448730_at	Cpa3	2.3	1450648_s_at	H2-Ab1	-2.1
1450344_a_at	Ptger3	2.3	1433428_x_at	Tgm2	-2.1
1418260_at	Hunk	2.3	1422010_at	Tlr7	-2.1
1415972_at	Marcks	2.3	1436364_x_at	Nfix	-2.1
1438169_a_at	Frmd4b	2.3	1427313_at	Ptgir	-2.1
1435172_at	Eomes	2.3	1436032_at	---	-2.1

1420364_at	Gpr87	2.3	1437277_x_at	Tgm2	-2.1
1416724_x_at	Tcf4	2.3	1425702_a_at	Enpp5	-2.1
1450764_at	Aoah	2.3	1438674_a_at	Sfswap	-2.2
1418912_at	Plxdc2	2.3	1421840_at	Abca1	-2.2
1448460_at	Acvr1	2.2	1451767_at	Ncf1	-2.2
1421415_s_at	Gcnt2	2.2	1437513_a_at	Serinc1	-2.2
1417163_at	Dusp10	2.2	1450336_at	Setd1a	-2.2
1448798_at	Eps8l3	2.2	1425570_at	Slamf1	-2.2
1417777_at	Ptgr1	2.2	1434062_at	Rabgap1l	-2.2
1448233_at	Prnp	2.2	1420342_at	Gdap10	-2.2
1416723_at	Tcf4	2.2	1421923_at	Sh3bp5	-2.3
1424733_at	P2ry14	2.2	1427511_at	---	-2.3
1425137_a_at	H2-Q10	2.2	1460251_at	Fas	-2.3
1435870_at	Chpt1	2.1	1425519_a_at	Cd74	-2.3
1425452_s_at	Fam84a	2.1	1425569_a_at	Slamf1	-2.4
1433558_at	Dab2ip	2.1	1418174_at	Dbp	-2.4
1434149_at	Tcf4	2.1	1451542_at	Ssbp2	-2.5
1417421_at	S100a1	2.1	1452416_at	Il6ra	-2.5
1433575_at	Sox4	2.1	1454675_at	Thra	-2.5
1417714_x_at	Hba-a1	2.1	1450048_a_at	Idh2	-2.5
1416129_at	Errfi1	2.1	1418398_a_at	Tspan32	-2.5
1435446_a_at	Chpt1	2.1	1422231_a_at	Tnfrsf25	-2.6
1449270_at	Plxdc2	2.1	1418126_at	Ccl5	-2.6
1450744_at	Ell2	2.1	1423466_at	Ccr7	-2.7
1456028_x_at	Marcks	2.1	1419696_at	Cd4	-2.8
1415971_at	Marcks	2.1	1436363_a_at	Nfix	-3.0
1421187_at	Ccr2	2.1	1416330_at	Cd81	-3.6

SUPPLEMENTAL REFERENCES

1. Trapnell C, Pachter L, and Salzberg SL. TopHat: discovering splice junctions with RNA-Seq. *Bioinformatics.* 2009;25(9):1105-11.
2. Anders S, Pyl PT, and Huber W. HTSeq--a Python framework to work with high-throughput sequencing data. *Bioinformatics.* 2015;31(2):166-9.
3. Anders S, and Huber W. Differential expression analysis for sequence count data. *Genome Biol.* 2010;11(10):R106.
4. Wang L, Wang S, and Li W. RSeQC: quality control of RNA-seq experiments. *Bioinformatics.* 2012;28(16):2184-5.
5. Markham NO, Cooper T, Goff M, Gribben EM, Carnahan RH, and Reynolds AB. Monoclonal antibodies to DIPA: a novel binding partner of p120-catenin isoform 1. *Hybridoma (Larchmt).* 2012;31(4):246-54.
6. Zhao Z, Condomines M, van der Stegen SJC, Perna F, Kloss CC, Gunset G, Plotkin J, and Sadelain M. Structural Design of Engineered Costimulation Determines Tumor Rejection Kinetics and Persistence of CAR T Cells. *Cancer Cell.* 2015;28(4):415-28.